Elektrotechnik & Informationstechnik (2016) 133/3: 183–190. DOI 10.1007/s00502-016-0407-9

SIMO UHF RFID reader using sensor fusion for tag localization in a selected environment

L. Görtschacher, J. Grosinger, H. N. Khan, B. Auinger, D. Amschl, P. Priller, U. Muehlmann, W. Bösch

This paper presents an ultra high frequency (UHF) radio frequency identification (RFID) reader for transponder (tag) localization in a selected environment—an AVL engine test bed. The choice of the UHF RFID reader hardware components is based on the evaluation of radio channel measurements in the engine test bed. The presented method of the channel measurement based implementation of an RFID reader can be favorably applied to realize reliable custom-built UHF RFID systems in any selected environment. The core of the implemented UHF RFID reader is a software defined radio (SDR) that enables rapid prototyping and thus a fast verification of localization techniques. The localization is realized by a single input multiple output (SIMO) antenna configuration and the exploitation of phase difference of arrival (PDoA) techniques. The implemented PDoA techniques allow to estimate the direction and the range of a tag. A sensor fusion of direction and range estimates enables a two dimensional tag localization. The functionality of the reader hardware implementation and the implemented PDoA techniques have been verified in an anechoic chamber reaching a localization accuracy of 15 cm.

Keywords: phase difference of arrival; sensor fusion; software defined radio; tag localization; UHF RFID

SIMO UHF RFID-Lesegerät zur Tag-Lokalisierung mittels Sensorfusion in einer ausgewählten Umgebung.

Dieser Artikel präsentiert ein RFID (Radio Frequency Identification)-Lesegerät im UHF (Ultra High Frequency)-Frequenzbereich, das die Lokalisierung von RFID-Transpondern (Tags) in einer ausgewählten Umgebung – einem AVL-Motorprüfstand – ermöglicht. Die Hardware-Komponenten des UHF RFID-Lesegerätes wurden auf der Grundlage einer Auswertung von Kanalmessungen im Motorprüfstand ausgewählt. Die präsentierte Methode zur Implementierung eines Lesegerätes aufgrund von Kanalmessungen kann für die Realisierung von zuverlässigen speziell angefertigten UHF RFID-Systemen in jeder ausgewählten Umgebung angewendet werden. Als Kern des Lesegerätes fungiert ein softwaregesteuertes Sende- und Empfangsgerät (SDR, Software Defined Radio), welches eine schnelle Prototypenentwicklung sowie eine schnelle Verifikation der Lokalisierungstechniken erlaubt. Die Lokalisierung wird durch eine spezielle Antennenanordnung (SIMO, Single Input Multiple Output) und den Einsatz spezieller PDoA (Phase Difference of Arrival)-Lokalisierungstechniken ermöglicht. Die implementierten PDoA-Techniken basieren auf der Messung von Phasendifferenzen der vom Tag zurückgestreuten Hochfrequenzsignale und erlauben eine Schätzung der Richtung und des Abstands eines Tags. Durch die Fusion von Richtungs- und Abstandsschätzungen wird eine zweidimensionale Lokalisierung der Tags erreicht. Die Funktionalität des Lesegerätes und der implementierten PDoA-Techniken wurde in einer reflexionsfreien Kammer verifiziert, wobei eine Lokalisierungsgenauigkeit von 15 cm erreicht wurde.

Schlüsselwörter: Phase Difference of Arrival; Sensorfusion; Software Defined Radio; Tag-Lokalisierung; UHF RFID

Received April 11, 2016, accepted April 29, 2016, published online May 25, 2016

1. Introduction

In backscatter radio frequency identification (RFID) systems, the objects that have to be identified are equipped with RFID transponders (tags). The tags modulate the backscattered signal that was sent by an interrogator (reader) [1]. Especially, in applications with a plurality of objects to be identified, the use of batteryless, or rather passive tags is very economical, as they are low cost and low maintenance devices [1]. The possibility of using the backscatter RFID technology not only for the identification of objects but also for the localization of these objects, has led to the proposal of several new applications in recent years. A small excerpt of the possible applications is the localization of pallets in warehouses [2], the localization of misplaced books in libraries [3], and the localization of every day products in smart homes [4]. However, the performance of a backscatter RFID system and its localization capabilities strongly depend on the environment where it is used in. Operating RFID systems in metallic environments suffers from multipath propagation of the radio signals. Consequences of this multipath propagation are the distorted power transfer to the passive tags at some regions as well as the reception of distorted tag signals at the reader leading to a distorted

Görtschacher, Lukas, Institute of Microwave and Photonic Engineering, Graz University of Technology, Inffeldgasse 12, 8010 Graz, Austria (E-mail: lukas.goertschacher@tugraz.at); **Grosinger, Jasmin,** Institute of Microwave and Photonic Engineering, Graz University of Technology, Inffeldgasse 12, 8010 Graz, Austria; **Khan, Hasan Noor,** Institute of Microwave and Photonic Engineering, Graz University of Technology, Inffeldgasse 12, 8010 Graz, Austria; **Auinger, Bernhard,** Institute of Microwave and Photonic Engineering, Graz University of Technology, Inffeldgasse 12, 8010 Graz, Austria; **Amschl, Dominik,** Institute of Microwave and Photonic Engineering, Graz University of Technology, Inffeldgasse 12, 8010 Graz, Austria; **Priller, Peter,** AVL LIST GmbH, Hans-List-Platz 1, 8020 Graz, Austria; **Muehlmann, Ulrich,** NXP Semiconductors Austria, Mikron-Weg 1, 8101 Gratkorn, Austria; **Bösch, Wolfgang,** Institute of Microwave and Photonic Engineering, Graz University of Technology, Inffeldgasse 12, 8010 Graz, Austria

localization. Several localization approaches have been proposed in recent years to combat these distortions that differ in terms of localization accuracy, implementation effort, and material costs. These approaches reach from using systems (e.g., ultra wide band system [5], frequency modulated continuous wave system [6]) parallel to an RFID system over the use of reference tags [7] and multiple input multiple output systems [8] up to RFID signals with superimposed spread spectrum signals [9].

Our approach is to implement a narrow band and low cost UHF RFID localization system that does not rely on the use of reference tags. A channel measurement based system hardware dimensioning assures a sufficient power transfer to the tags and thus a reliable communication in a selected environment. In order to combat distorted localization in multipath environments, the localization system exploits the use of three operating frequencies. In particular, this paper presents an RFID reader for tag localization in an AVL engine test bed. The starting point for the reader implementation is a measurement based characterization of the radio channel in this engine test bed. Generally, this approach allows a decoupled examination of the radio channel and the RFID system components and thus the exploration of the individual influence of various RFID system components (different tag and reader parameters) on the system performance in selected environments. For the reader implementation presented here, the channel measurements are used to estimate the minimum reader hardware requirements—with respect to the radio signal power (minimum transmit power, etc.)—that are necessary to perform a reliable tag localization in the engine test bed. The final reader implementation exploits phase difference of arrival (PDoA) techniques for the localization of RFID tags as they are more robust in multipath environments compared to state-of-the-art techniques that are based on the received signal strength [10]. For the exploitation of the PDoA techniques, the reader antennas are setup in a single input multiple output (SIMO) configuration. The core of the reader is a software defined radio (SDR) that makes the reader flexible in order to achieve a rapid prototyping and a fast verification of the implementation.

The paper is structured as follows. Section 2 describes the communication links of the used SIMO RFID system. Section 3 shows the RFID system feasibility in the AVL engine test bed by assuming state-of-the-art system components. The reader implementation is presented in Sects. 4 and 5 and is based on the evaluation of the channel measurements in the engine test bed. Sections 6 and 7 present the functional verification of the implemented reader and the conclusions, respectively.

2. SIMO RFID system

A backscatter RFID system can be classified into three communication links, the forward link, the backward link, and the backscatter link. In the forward link, the reader consecutively sends commands and a continuous wave (CW) signal to the tag that consists of an antenna and a chip. The CW signal provides the power for the tag that is necessary to supply its chip. Once the tag has received enough power, it starts to modulate the backscattered signal with its information depending on the reader command, e.g., its identification number ID. This link from the tag to the reader is denoted as backward link. If the backscattered tag signal can be correctly interpreted by the reader, the RFID system is reliable. The backscatter link describes the combination of the forward link and the backward link (reader-tag-reader) [1]. The reliability of a backscatter RFID system strongly depends on the signal power within the mentioned communication links. The minimum power of the CW signal received at the tag is limited by the sensitivity of the tag chip (chip sensitivity).

Fig. 1. SIMO antenna configuration: The spacing of TX and RX_1 is 60 cm, while the spacing of TX and RX_2 is 90 cm

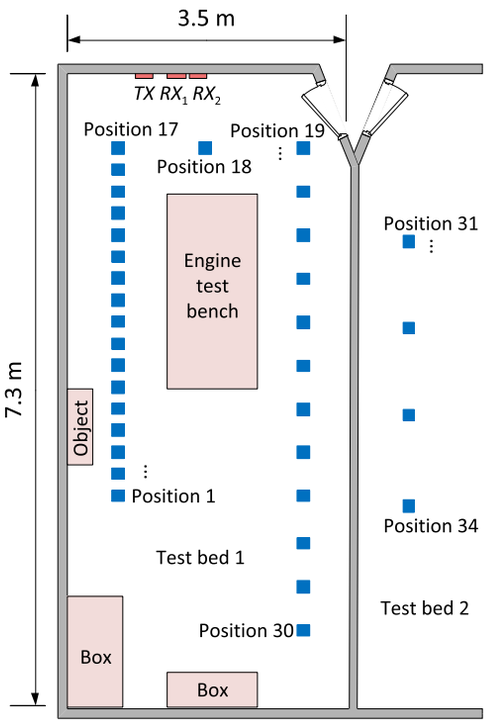

Fig. 2. AVL engine test bed floor plan: Test bed 1 consists of metallic walls and several metallic objects like the engine test bench, boxes and objects. The reader antennas are mounted on the window to the control room of test bed 1. For the measurements, the tag antenna has been positioned at several points in test bed 1 (positions 1 to 30). Also, interference measurements have been performed by positioning the tag antenna in the neighboring test bed 2 (positions 31 to 34)

The minimum power of the tag signal received at the reader is limited by the sensitivity of the reader receiver (reader sensitivity) [11].

As mentioned above, the UHF RFID reader is based on a SIMO antenna configuration, consisting of one transmitting antenna TX and two receiving antennas RX_1, RX_2 of the type Motorola AN480 [12] (see Fig. 1). As a result of the SIMO configuration, the communication links expand to one forward link FL, two backward links BL_1, BL_2 and two backscatter links BSL_1, BSL_2.

3. System reliability

The reliability of implementing a SIMO RFID system performing tag localization in the engine test bed at AVL is in the following investigated with respect to the signal power and state-of-the-art RFID system parameters. The investigation is based on channel measurements that characterize the communication links within this challenging multipath environment. In particular, the system reliability is investigated with respect to the measured power availability in the communication links at 890 MHz [11, 13]. Figure 2 shows the

floor plan of the AVL engine test bed (test bed 1) and a neighboring engine test bed (test bed 2). The reader antennas (TX, RX_1, RX_2) have been mounted on a window to the control room of test bed 1 at a height of 1.5 m. For the measurement of the communication links, a tag antenna has been positioned at several positions within test bed 1 (positions 1 to 30) at the same height as the reader antennas. To investigate the interference of tags that are located in neighboring engine test beds, additional measurements have been performed where the tag antenna has been positioned in test bed 2 (positions 31 to 34). Two different scenarios have been considered for the measurement of the power in the communication links. For the tag antenna, a custom built patch antenna—with typical tag antenna gain—has been used in the tag scenario, while a Motorola AN480 antenna—the same as for the reader antennas—has been used as the tag antenna in the reference scenario. The measurements of the reference scenario are used to obtain a best case scenario in test bed 1 and a worst case scenario in test bed 2.

The channel measurements have been performed by measuring the scattering (S) parameters with a vector network analyzer (VNA) [14]. For every tag position, the S parameters have been measured 20 times in a frequency range from 700 MHz to 1200 MHz. The reference plane for the measurements has been set to the input of the antennas. Consequently, the antennas are part of the measured channel. The communication links of the system are described by the transmission coefficients of the S parameters. The amount of power that is transmitted at a certain frequency from one to another antenna, or rather the channel gain can be calculated as the squared magnitude of the transmission coefficients. The backscatter link channel gain g_{BSL} is the sum of the forward link channel gain g_{FL} and the backward link channel gain g_{BL} ($g_{BSL}|_{dB} = g_{FL}|_{dB} + g_{BL}|_{dB}$) [11].

3.1 Evaluation method

The system reliability is determined by combining the knowledge of the measured communication links and specified RFID system parameters [13]. More precisely, the measured channel gain of the communication links at 890 MHz is compared to channel gain thresholds that are defined by the RFID system components (reader and tag parameters). The evaluation is based on 600 (30 positions in test bed 1 times 20 repetitions) measurement points in the reference and tag scenarios and 80 (4 positions in test bed 2 times 20 repetitions) measurement points in the interference reference scenario. Here, the feasibility of the system is evaluated with respect to state-of-the-art RFID system parameters. For the RFID reader, a transmission power of $P_{TX} = 30$ dBm and a sensitivity of $T_{RX} = -105$ dBm for both receivers are assumed (Zebra FX9500 RFID Reader [15]). The tag provides a chip sensitivity of $T_{Chip} = -17.5$ dBm (NXP UCODE G2iM [16]), a modulation efficiency of $\eta = -7$ dB (amplitude modulation [17]) and a power transmission coefficient of $\tau = 0$ dB. $\tau = 0$ dB means a perfect matching between tag antenna and tag chip. The measured matching of the antennas (reflection coefficients) allows the latter assumption. The antenna matching is -13 dB in the tag scenario and -20 dB in the reference scenario. The above mentioned state-of-the-art parameters lead to a forward link threshold F_{Th} and to a backscatter link threshold B_{Th} for both backscatter links of [11]:

$$F_{Th} = T_{Chip} - \tau - P_{TX} = -47.5 \text{ dB} \quad \text{and} \tag{1}$$

$$B_{Th} = T_{RX} - \eta - P_{TX} = -128 \text{ dB}. \tag{2}$$

The RFID system is forward link limited, if the forward link channel gain is lower than F_{Th}. The system is denoted as backward link limited, if the forward link channel gain is higher than F_{Th}, but the backscatter link channel gain is lower than B_{Th} [10].

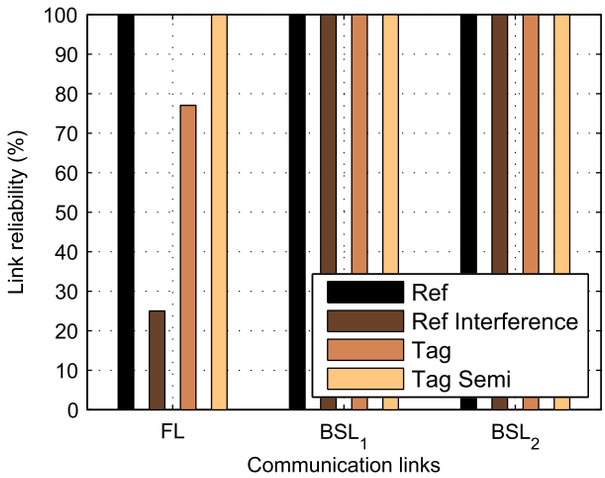

Fig. 3. System feasibility: The system feasibility of the reference and the tag scenario is depicted by the reliability of their communication links. The communication links of the reference scenario (*Ref*) are 100 % reliable, while the system is forward link limited in the tag scenario (*Tag*). The possibility for detecting an interfering tag is 25 % in the worst case (*Ref Interference*). The forward link limitation at some positions in the room in the tag scenario can be overcome for example by using semi passive tags (*Tag Semi*)

3.2 Evaluation

The system reliability of the two mentioned scenarios is evaluated by means of the reliability of the individual communication links (FL, BSL_1, BSL_2). The reliability of the communication links is indicated in percent and is illustrated by means of bar charts (see Fig. 3). The forward link is 100 % reliable, if g_{FL} is higher than F_{Th}, while the backscatter link is 100 % reliable, if g_{BSL} is higher than B_{Th}, for every measured tag position. However, the system is only 100 % reliable, if FL, BSL_1, and BSL_2 are 100 % reliable and thus, the system is neither forward link limited nor backward link limited.

Figure 3 shows the reliability of the communication links for the reference (Ref, Ref Interference) and the tag (Tag) scenario. The communication links in the reference scenario in test bed 1 (Ref) are 100 % reliable and thus, the system is 100 % reliable in this best case scenario. The interference measurements (Ref Interference) exhibit 25 % reliability of the forward link and 100 % reliability of the backscatter links. This results in the detection of an interfering tag with a probability of 25 % in this worst case. However, by reducing the reader transmission power by 2 dB ($P_{TX} = 28$ dBm), no interferences occur anymore, while the system still operates reliable in test bed 1. In the tag scenario (Tag), the forward link is 77 % reliable, while both backscatter links are 100 % reliable. Thus, the tag does not receive enough power at some positions to respond. This problem can be overcome by using battery-assisted, or rather-semi passive RFID tags with higher chip sensitivities. Figure 3 shows that using semi-passive tags (Tag Semi) with a chip sensitivity of $T_{Chip} = -40$ dBm (Intelleflex XC3 IC [18]) leads to a 100 % reliable system. However, using battery-assisted tags would increase the acquisition and maintenance cost of the localization system. The future goal is to exploit the advantages of passive tags. Thus, the placement of the reader antennas has to be chosen carefully to increase their coverage in the test bed.

Additionally, the system reliability is investigated with respect to the influence of varying the tag antenna height and the influence of a running test engine. The respective measurements have been repeated at 5 tag positions (1, 17, 18, 19, 27) in the tag scenario. First,

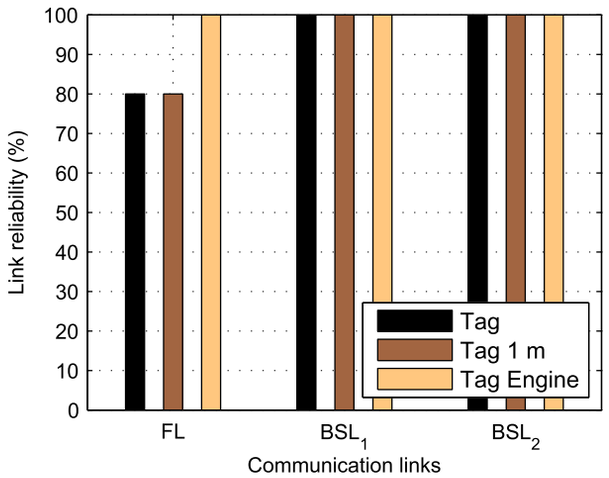

Fig. 4. Link reliability comparison of measurements with different conditions in the tag scenario at 5 tag positions (1, 17, 18, 19, 27): Varying the tag antenna height and the influence of a running test engine do not degrade the link reliability. The differences in the forward links can be explained by slightly differing tag antenna positions due to manual positioning of the tag antenna

the height of the tag antenna has been reduced to 1 m (Tag 1 m) and second, a test engine has been run in test bed 1 (Tag Engine). Figure 4 shows a comparison of the link reliability in the tag scenario with the three different measurement conditions, i.e., Tag, Tag 1 m and Tag Engine at the 5 tag positions. For Tag and Tag 1 m, the tag does not receive enough power at one position to respond (80 % reliability of the forward links), while no limitations can be observed for Tag Engine. The differences can be explained by slightly differing tag antenna positions caused by the manual positioning. However, no degradation of the system can be observed by changing the measurement conditions in the tag scenario.

4. Reader hardware implementation

The previous section investigates the system reliability in the AVL engine test bed with respect to state-of-the-art RFID system parameters, while this section presents the SIMO UHF RFID reader hardware implementation based on the performed channel measurements. For the implementation, some hardware requirements have to be considered in order to perform a reliable localization in the AVL engine test bed. On the one hand, the reader has to fulfill requirements with respect to the signal power in the communication links, i.e., the reader has to provide a sufficient transmission power and sensitivity. On the other hand, the reader has to fulfill requirements in order to perform localization based on phase difference of arrival (PDoA) techniques [10]. The core of the reader is chosen to be an SDR, to guarantee a fast implementation of the hardware and the PDoA algorithms. In the following, a estimation of the requirements for the SDR and additional hardware components is presented. Especially, the tag scenario using semi-passive tags with a chip sensitivity of $T_{\text{Chip}} = -40$ dBm is assumed for these considerations.

4.1 Minimum transmission power

A minimum transmission power $P_{\text{TX,min}}$ of the reader is required to provide the tag with sufficient power at all positions in test bed 1. $P_{\text{TX,min}}$ is determined by the minimum channel gain of the forward link $g_{\text{FL,min}}$ at 890 MHz and the tag parameters, i.e., the chip sensitivity and the power transmission coefficient. The minimum transmission power is [11],

$$P_{\text{TX,min}} = T_{\text{Chip}} - \tau - g_{\text{FL,min}} = 24.5 \text{ dBm}, \tag{3}$$

with a minimum measured channel gain of $g_{\text{FL,min}} = -64.5$ dB and a power transmission coefficient of $\tau = 0$ dB.

4.2 Minimum reader sensitivity

To correctly detect the backscattered tag signals from all tag positions in test bed 1, the reader has to provide a minimum reader sensitivity $T_{\text{RX,min}}$. $T_{\text{RX,min}}$ is determined by the minimum measured channel gain of the backscatter links $g_{\text{BSL,min}}$, the reader transmission power, and the modulation efficiency of the tag. For the following, only the minimum transmission power of $P_{\text{TX,min}} = 24.5$ dBm is used for the calculations to obtain a lower bound of the reader requirements. With a minimum measured channel gain of $g_{\text{BSL,min}} = -114$ dB and a modulation efficiency of $\eta = -7$ dB, the minimum reader sensitivity is calculated as [11],

$$T_{\text{RX,min}} = P_{\text{TX,min}} + g_{\text{BSL,min}} + \eta = -96.5 \text{ dBm}. \tag{4}$$

Providing this sensitivity means that signals with a minimum power of −96.5 dBm can be resolved at the reader. From this it follows that the weakest signals at the reader receiver have an amplitude of about 150 µV, assuming a 50 Ω system and a gain of 31.5 dB of a low noise amplifier in the receiving chain of the reader [1]. Thus, at least 12 bit analog to digital converters (ADCs) are necessary to detect a change of the amplitude modulated tag signal at the receiver, when assuming a full scale range of 1 V [19]. This is only a rough estimation not taking any losses in the receiving chains into account.

4.3 PDoA-related requirements

The SDR has to fulfill some requirements for the exploitation of PDoA techniques. As the SIMO configuration of the reader antennas is necessary to perform spatial domain (SD)-PDoA techniques (see Sect. 5.2), the SDR has to provide at least one transmitting chain and two receiving chains. For detecting phase differences of the signals that are received at the two receiving antennas, it is important that the receiving chains provide phase coherence and phase alignment [10].

4.4 Final reader setup

Based on the mentioned hardware requirements, a SDR from National Instruments (NI USRP-2942R [20]) has been chosen that fulfills almost all requirements. It is a 2 × 2 MIMO system and hence provides two separate transmitting chains and two separate receiving chains. It can operate in a full duplex mode (transmitting and receiving at the same time) and provides 14 bit ADCs. The maximum output power of the SDR is 17 dBm (measured). The two receiving chains are phase coherent, but not phase aligned. However, this phase misalignment can be corrected by an initial calibration (see Sect. 5.1). The final RFID reader is composed of the NI USRP-2942R SDR and the necessary additional hardware components to meet the requirements (see Fig. 5). A switch matrix is used to perform an initial automatic calibration of the two receiver chains of the SDR, i.e., to measure the phase misalignment of the receiving chains. A power amplifier increases the transmission signal to a sufficient power level. A laptop computer controls the hardware components of the reader and processes the raw inphase (I) and quadrature (Q) data received from the SDR. One transmitting antenna and two receiving antennas complete the setup of the SIMO UHF RFID reader.

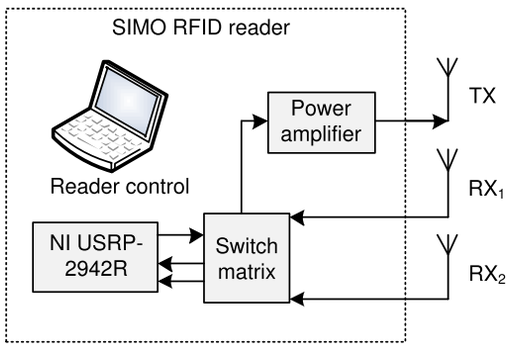

Fig. 5. Final SIMO UHF RFID reader setup: The reader is composed of the SDR (NI USRP-2942R), the switch matrix, the power amplifier, one transmitting antenna and two receiving antennas and is controlled by the laptop computer (reader control)

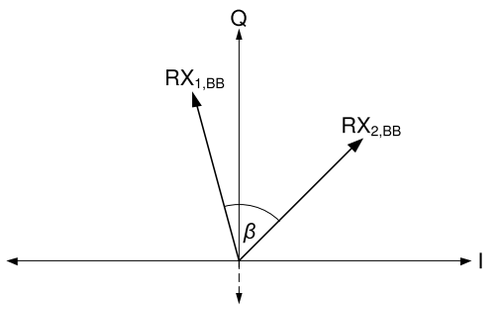

Fig. 6. Determination of the phase misalignment: When receiving the same CW signal at both receivers, the angle β between the baseband vectors $RX_{1,BB}$ and $RX_{2,BB}$ is equivalent to the phase misalignment

5. Reader software implementation

The previous section presented the reader implementation with respect to hardware aspects. This section deals with the procedure of the initial calibration, the implementation of the PDoA algorithms, and the sensor data fusion. For the two dimensional localization of tags, two PDoA algorithms are implemented that estimate the direction (SD-PDoA) and the range (frequency domain (FD)-PDoA) of the tag, respectively. The definitions of the estimators are based on the assumption that the tag is far away from the reader, compared to the spacing of the receiving antennas, the tag is at rest within the time period of an estimation, and the tag is frequency independent within the range of the operating frequencies [10].

5.1 Initial calibration

As stated in Sect. 4.4, the receiving chains are not phase aligned. However, this phase misalignment can be measured in advance and afterwards be incorporated into the localization estimates. The phase misalignment measurement is done in an automatic initial calibration phase. In this phase, the switch matrix switches the transmitting port via a splitter to both receiving ports. Thus, the same CW signal is provided to the two receiving chains of the SDR and allows to determine the phase misalignment. Figure 6 exemplarily shows the baseband IQ vectors $RX_{1,BB}$ and $RX_{2,BB}$ of the received signals at both receiving ports. The angle β between $RX_{1,BB}$ and $RX_{2,BB}$ is equivalent to the phase misalignment of the receiving chains. The system is calibrated by rotating $RX_{2,BB}$ by β towards $RX_{1,BB}$ and phase differences can be correctly detected.

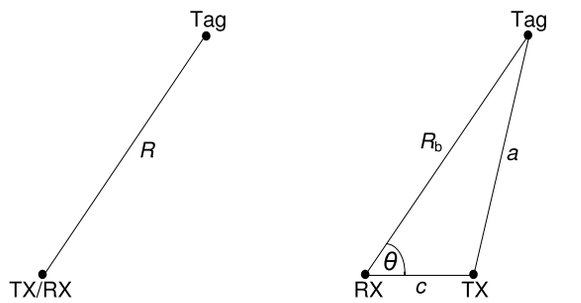

(a) Monostatic configuration (b) Bistatic configuration

Fig. 7. Range estimation: The range estimation in the monostatic configuration is based on the bisection of the distance TX/RX-Tag-TX/RX. In the bistatic configuration, the range estimation is based on the calculation of side R_b of the triangle, where the direction estimate Θ is an angle of the triangle

5.2 Localization estimators

The direction estimator Θ is based on different path lengths of the backscattered tag signal received at the two receiving antennas at a certain frequency. The different path lengths cause a phase difference $\Delta\varphi_D$ of the two signals that is related to the direction of the tag, where the reference point is in the center of the receiving antennas. Θ can be calculated by using a trigonometric relationship as [10],

$$\Theta = \cos^{-1} \frac{c}{2\pi f} \frac{\Delta\varphi_D}{d}, \tag{5}$$

where c is the light velocity, f the operating frequency and d the distance between the receiving antennas.

The range estimator R is based on the phase difference $\Delta\varphi_R$ of two consecutively received tag signals at different operating frequencies at one receiving antenna. Assuming a monostatic antenna configuration, i.e., one antenna for transmission and reception, R can be calculated as [10],

$$R = \frac{c}{4\pi} \frac{\Delta\varphi_R}{\Delta f}, \tag{6}$$

where Δf is the frequency difference of the operating frequencies. For a monostatic antenna configuration, the estimator R is based on the fact that half of $\Delta\varphi_R$ transpires in the backward link (see Fig. 7a). This fact does not hold for the SIMO RFID reader presented here and Eq. (6) would lead to imprecise estimates. As transmitting and receiving antennas are in a bistatic configuration, the estimation of the range expands to the calculation of the side R_b of a triangle (see Fig. 7). Figure 7b depicts the triangle formed by TX, the tag, and RX and the sides a, R_b, and c, where RX is the reference point in the center of RX_1 and RX_2. We assume that the sum of the triangle sides a and R_b is approximately given by $2 \cdot R$, i.e., $a + R_b \approx 2 \cdot R$ (as the reference point is not exactly at a receiving antenna). By incorporating the knowledge of the tag direction estimate Θ that is an angle of the triangle, the range in the bistatic configuration R_b can be calculated by rearranging the law of cosines as,

$$R_b = \frac{c^2 - 4R^2}{2c\cos\Theta - 4R}. \tag{7}$$

5.3 Sensor data fusion

The reader is implemented to operate at three different operating frequencies f_0, f_1, and f_2 in order to make the tag localization

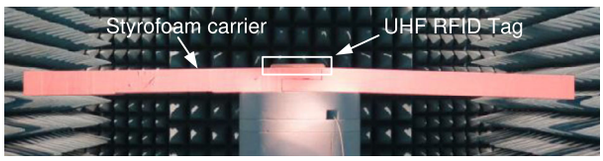

Fig. 8. Test setup in the anechoic chamber: The tag is positioned on a styrofoam carrier in the middle of the chamber. Tag and reader antennas are at the same height

more robust in multipath environments [21]. The reader consecutively sends commands at the different operating frequencies and stores the received data for the post processing. This procedure leads to three direction estimates Θ_0, Θ_1, Θ_2 and to two range estimates for each receiving antenna $R_{\Delta f_1,\mathrm{RX}_j}$, $R_{\Delta f_2,\mathrm{RX}_j}$, where $\Delta f_1 = f_1 - f_0$ and $\Delta f_2 = f_2 - f_0$. A fusion of the estimated direction and range data of the RFID tag leads to the final two dimensional localization capability of the implemented RFID reader. However, the reader observes the estimates for a period of time and then statistically evaluates the data. The most trustful estimates of the direction (Θ_0, Θ_1 or Θ_2) and the range ($R_{\Delta f_1,\mathrm{RX}_j}$ or $R_{\Delta f_2,\mathrm{RX}_j}$), i.e., the estimates with the smallest standard deviation are fused to find the most probable tag position.

6. Reader verification

The functionality of the implemented reader has been verified in an anechoic chamber. The anechoic environment especially allows the evaluation of the reader software implementation, i.e., the initial calibration phase, the PDoA algorithms, and the sensor data fusion. For the measurements, a passive tag (Sokymat InLine UHF Tag [22]) was placed on a styrofoam carrier in the middle of the anechoic chamber at the same height as the reader antennas (see Fig. 8).

Figure 9 shows the coordinates of the tag positions (true pos.) in the anechoic chamber, where the center of the reader receiving antennas is the origin of the coordinate system. The position of the tag has been estimated in 20 cm steps for a fixed x coordinate (vert. pos.) on the one hand and for a fixed y coordinate (hor. pos.) on the other hand. The adjustable operating frequencies have been set to $f_0 = 869$ MHz, $f_1 = 866$ MHz, and $f_2 = 872$ MHz. The shown position estimates are composed of the direction estimate Θ_0 and the mean of the range estimates $R_{\Delta f_2,\mathrm{RX}_1}$ and $R_{\Delta f_2,\mathrm{RX}_2}$ ($\Delta f_2 = 3$ MHz). The maximum deviation of the position estimate to the true position is about 15 cm. The estimation errors can be explained by a combination of the following reasons. The manual placement of the tag introduces slight deviations from the true positions. Small errors may be introduced by deviations of the generated operating frequencies. The assumptions for the definition of the estimators that are mentioned in Sect. 5 do not completely hold for this environment, e.g., the tag is not far away from the reader, compared to the spacing of the receiving antennas. Finally, the range estimation is based on not faultless direction estimates [23].

7. Conclusions

This paper presents a method for implementing a custom-built UHF RFID reader for tag localization for the use in a specific environment that is in our case an AVL engine test bed. The method is based on radio channel measurements in the engine test bed that allows the determination of reader hardware requirements for the implementation of a reliable tag localization system. The final reader hardware implementation is able to perform reliable localization in the engine test bed with respect to power availability in the radio channel. The

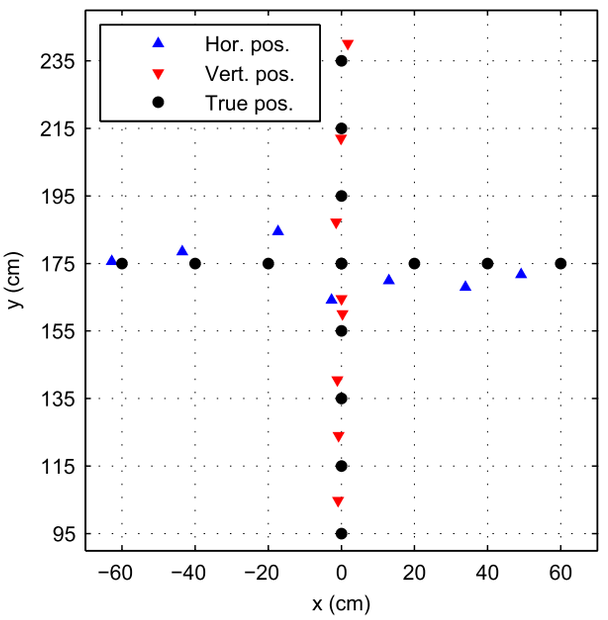

Fig. 9. Functional verification in the anechoic chamber: The true and the estimated positions show a maximum deviation of 15 cm. The position estimates are composed of Θ_0 and the mean of $R_{\Delta f_2,\mathrm{RX}_1}$ and $R_{\Delta f_2,\mathrm{RX}_2}$

localization capability of the reader is provided by the exploitation of PDoA techniques. This first prototype of the reader achieves a localization accuracy of 15 cm in an anechoic chamber. Recently, the localization capability of the realized reader was demonstrated within an AVL engine test bed. The demonstration showed that the position of a passive tag can be correctly assigned to one of four equally sized regions in the test bed, i.e., detecting in which of the four regions the tag is located. The reader operates at three different operating frequencies to make the tag localization more robust in difficult multipath environments. In the future, the localization robustness will be improved by exploiting more than three operating frequencies [21]. In addition, the implemented SDR based RFID reader can be favorably exploited for the prototyping of future RFID systems, e.g. RFID systems that can detect sensor information of passive RFID tags in addition to their ID and location [24].

Acknowledgements

This work was performed as part of the K-project "Secure Contactless Sphere—Smart RFID Technologies for a Connected World" that was funded by the Austrian Research Promotion Agency (FFG).

References

1. Dobkin, D. M. (2012): The RF in RFID: UHF RFID in practice. Burlington: Newnes.
2. Zhou, J. R., Zhang, H. J., Zhou, H. L. (2015): Localization of pallets in warehouses using passive RFID system. J. Cent. South Univ. Technol., 22, 3017–3025.
3. Wang, J., Katabi, D. (2013): Dude, where's my card? RFID positioning that works with multipath and non-line of sight. Comput. Commun. Rev., 43(4), 51–62.
4. Fortin-Simard, D., et al. (2015): Exploiting passive RFID technology for activity recognition in smart homes. IEEE Intell. Syst., 30(4), 7–15.

5. Arnitz, D., Muehlmann, U., Witrisal, K. (2010): UWB ranging in passive UHF RFID: proof of concept. Electron. Lett., 46(20), 1401–1402.
6. Ussmueller, T., et al. (2012): A multistandard HF/UHF-RFID-tag with integrated sensor interface and localization capability. In Proc. IEEE international conference on RFID, RFID (pp. 66–73). New York: IEEE Press.
7. Nick, T., et al. (2011): Localization of UHF RFID labels with reference tags and unscented Kalman filter. In Proc. IEEE international conference on RFID-technologies and applications, RFID-TA (pp. 168–173). New York: IEEE Press.
8. Scherhaufl, M., Pichler, M., Stelzer, A. (2015): UHF RFID localization based on evaluation of backscattered tag signals. IEEE Trans. Instrum. Meas., 64(11), 2889–2899.
9. Arthaber, H., Faseth, T., Galler, F. (2015): Spread-spectrum based ranging of passive UHF EPC RFID tags. IEEE Commun. Lett., 19(10), 1734–1737.
10. Nikitin, P. V., et al. (2010): Phase based spatial identification of UHF RFID tags. In Proc. IEEE international conference on RFID (pp. 102–109). New York: IEEE Press.
11. Grosinger, J. (2013): Feasibility of backscatter RFID systems on the human body. EURASIP J. Embed. Syst., 2013(2), 1–10.
12. Motorola (2015): RFID antenna family. Online: http://www.barcodesinc.com/pdf/Motorola/an-series.pdf, May 2015.
13. Görtschacher, L., et al. (2015): SIMO RFID system performance in an engine test bed. In Proc. international EURASIP workshop on RFID technology, EURFID (pp. 120–125). New York: IEEE Press.
14. Molisch, A. F. (2007): Wireless communications. New York: Wiley.
15. Zebra Technologies (2015): Zebra FX9500 fixed RFID reader. Online: www.zebra.com/us/en/products/rfid/rfid-readers/fx9500/fx9500_spec_sheet.html, May 2015.
16. NXP Semiconductors (2015): SL3S1003_1013. Online: www.nxp.com/documents/data_sheet/SL3S1003_1013.pdf, May 2015.
17. Rembold, B. (2009): Optimum modulation efficiency and sideband backscatter power response of RFID-tags. Frequenz, 63(1–2), 9–13.
18. Intelleflex (2015): The Intelleflex XC3 technology platform. Online: www.intelleflex.com/Products.RFID.Technology.Overview.asp, May 2015.
19. Kester, W., et al. (2003): Mixed-signal and DSP design techniques. Burlington: Newnes.
20. National Instruments (2016): NI USRP 2942R. Online: http://www.ni.com/datasheet/pdf/en/ds-538.
21. Li, X., Zhang, Y., Amin, M. G. (2009): Multifrequency-based range estimation of RFID tags. In Proc. IEEE international conference on RFID (pp. 147–154). New York: IEEE Press.
22. Sokymat (2016): InLine UHF tag ucode EPC Gen2 869 MHz. Online: http://www.rfid-webshop.com/shop/download/tags/UHF868_915MHz/Sokymat/I&L/UHF/.
23. Görtschacher, L., et al. (2016): SDR based RFID reader for passive tag localization using phase difference of arrival techniques. In IEEE MTT international microwave symposium (IMS). Accepted for publication.
24. Grosinger, J., Görtschacher, L., Bösch, W. (2016): Sensor add-on for batteryless UHF RFID tags enabling a low cost IoT infrastructure. In IEEE MTT international microwave symposium (IMS). Accepted for publication

Authors

Lukas Görtschacher
studied electrical engineering at the Graz University of Technology, Austria. His M.Sc. thesis deals with the design and development of an antenna transducer for a backscatter radio frequency identification (RFID) sensor tag. He received his Dipl.-Ing. (M.Sc.) degree with honors in 2014. Since 2014, he has been working as a project assistant at the Institute of Microwave and Photonic Engineering at the Graz University of Technology and pursues a Ph.D. degree. His research area is RFID technologies, especially focused on localization and sensing.

Jasmin Grosinger
studied telecommunications at the Vienna University of Technology, Austria. In 2008, she received her Dipl. -Ing. (M.Sc.) degree with honors. From 2008 to 2013, she worked as a project assistant at the Institute of Telecommunications, Vienna University of Technology. There she worked on various projects dealing with radio frequency identification (RFID) technologies. In 2011, she was a lab associate at Disney Research in Pittsburgh, USA, working on backscatter RFID sensors. In 2012, she received her Dr. techn. (Ph.D.) degree with honors from Vienna University of Technology. In her Ph.D. thesis, she examined backscatter radio frequency systems and devices for novel wireless sensing applications. Since 2013, she has been working as a post doctorand at the Institute of Microwave and Photonic Engineering at Graz University of Technology and heads the research group RFID Technologies. Dr. Grosinger published more than 30 peer-reviewed publications and holds one US patent. She is actively involved in technical program committees of various RFID-related conferences and is associate editor of the IET Microwaves, Antennas & Propagation journal.

Hasan Noor Khan
did his B.Sc. in electrical engineering at the University of Engineering and Technology in Lahore, Pakistan, in 2004. His major was electronics and communication. In his B.Sc. thesis, he deals with the design of an autonomous navigational mobile robot. In 2007, he was awarded with a fellowship of the National Engineering and Scientific Commission of Pakistan for his M.Sc. studies at the University of Engineering and Technology in Lahore. His major was again in the field of electronics and communication. He did his M.Sc. thesis in the field of chaos-based spread spectrum communication systems. From February 2004 to April 2013, he was teaching extensively at different Pakistani universities. Since May 2013, he has been pursuing his Ph.D. degree at the Institute of Microwave and Photonic Engineering at the Graz University of Technology under a scholarship from the Higher Education Commission of Pakistan. His area of research is UHF RFID localization systems. He is on leave from the FAST-National University of Computer and Emerging Sciences Faisalabad, where he was serving as an Assistant Professor in the Electrical Engineering department.

Bernhard Auinger
received the master's degree in electrical engineering (Dipl. Ing.) in 2004 and the Dr. techn. degree with distinction in 2015, both from Graz University of Technology, Austria. From 2011 to 2015 he was involved in theoretical investigations for wireless communications and on test procedures for MIMO enabled user equipment using LTE, which was a cooperation between the Institute of Microwave and Photonic Engineering, Graz University of Technology, and the company Rohde & Schwarz, Munich, Germany. From 2005 to 2011 he initiated and led the electromagnetic compatibility group for automotive ICs at Philips Semiconductors and NXP Semiconductors. During his studies he was engaged in the comet mission

ROMAP/ROSETTA of the European Space Agency (ESA). Currently, he is researcher at the Institute of Electronics, Graz University of Technology, and investigates new semiconductor technologies and methods for increasing the efficiency, shrinking the unit size and reducing emissions of welding machines and switched power converters for solar power, also applying wireless communication theory in power electronics.

Dominik Amschl
was born in Graz, Austria. After a technical college (HTL) he started studying electrical engineering at Graz University of Technology. He is currently with the Institute of Microwave and Photonic Engineering of Graz University of Technology. His main task is performing radio frequency and mm-wave measurements at frequencies up to 110 GHz.

Peter Priller
is technology scout for embedded systems in AVL ITS Global Research & Technology.
After graduating in electrical engineering from the Graz University of Technology, Austria, he worked for some two years in ASIC development at an RFID startup. Since then he has been with AVL Graz in various positions from software development to system architecture/real-time systems to software project management. Since 2011 he has been in AVL ITS global R&T responsible for managing research co-operations and projects focusing on embedded systems and wired/wireless communication networks.

Ulrich Muehlmann
received his master's degree (Dipl.-Ing. in telematics) from the Graz University of Technology (TU Graz), Austria, in 2000. From 2000 to 2001 he attended the basic training course in the Austrian army. In 2001 he started research work in optical tracking at the Department of Electrical Measurement and Measurement Signal Processing (TU Graz). In November 2005 he received his Ph.D. degree (Dr. techn.) with honors. Since 2005 he has been with NXP Semiconductors (former Philips Semiconductors) working in the field of RFID/NFC technology focused on systems and analog innovation. He is author and/or co-author of several publications in the field of optical tracking, machine vision and RFID.
Ulrich Mühlmann is a member of several standardization bodies. In ETSI he is significantly involved in several groups (TG28, TG34) in the field of RFID/NFC spectrum mask engineering and channel management. He is also a member of CEPT/ECC working in the field of RFID spectrum management.

Wolfgang Bösch
In March 2010 Professor Dr. Wolfgang Bösch has joined the Graz University of Technology in Austria to establish a new Institute for Microwave and Photonic Engineering. Prior he has been the CTO of the Advanced Digital Institute in the UK, a not for profit organisation to promote research activities. Earlier he served as the Director of Business and Technology Integration for RFMD UK and for almost 10 years he has been with Filtronic plc as CTO of Filtronic Integrated Products and the Director of the Global Technology Group. Before joining Filtronic, he has held positions at the European Space Agency (ESA) working on amplifier linearization techniques, MPRTeltech in Canada working on MMIC technology projects and the Corporate R&D group of M/A-COM in Boston, USA where he worked on advanced topologies for high efficiency power amplifiers. For four years he was with DaimlerChrysler Aerospace (now Airbus) in Germany working on T/R Modules for airborne radar.
Professor Bösch received his engineering degrees from the Technical University of Vienna and Graz in Austria. He finalised his MBA with distinction at Bradford University School of Management in 2004. He is a Fellow of the IEEE and a Fellow of the IET. He published more than 80 papers and holds 4 patents. He was a Non- Executive Director of Diamond Microwave Devices (DMD) and the Advanced Digital Institute (ADI). He is currently a Non-Executive Director of VIPER-RF company in the UK.